35th Annual International Conference of the IEEE EMBS
Osaka, Japan, 3 - 7 July, 2013

The Role of Proprioceptive Feedback in Parkinsonian Resting Tremor

Nikhil Govil, Abraham Akinin, Samuel Ward, Joseph Snider, Markus Plank, Gert Cauwenberghs, and Howard Poizner.

Abstract— **In this paper we use a closed-loop force feedback system to investigate the effect of altering proprioceptive feedback on EEG and resting tremor in Parkinson's Disease. A velocity dependent counterforce simulating viscous friction was provided by haptic robots with simultaneous recording of kinematics, EMG and EEG while a patient was on and off dopaminergic medication. We were able to reduce the amplitude of the tremor. We also showed that force feedback shifts the center of EEG-EMG coherence posteriorly toward the somatosensory regions, which may have ramifications for noninvasive therapies.**

I. Introduction

Parkinsonian tremor is thought to result from central oscillators in the brain with projections to a wide number of cortical and subcortical regions [1]. Previous studies involving mechanical stimulation [2] and peripheral nerve stimulation [3] showed a modulation in the tremor frequency and amplitude from varying proprioceptive input. These studies did not show a consistent change in the tremor, but concluded that proprioception played a role in tremor genesis. High coherence between EEG and EMG during a tremor episode is present in the contralateral motor cortex area [4]. Fig. 1 shows the direction of the flow of information from the brain into kinematics. In the absence of visual and auditory feedback, proprioception is the only feedback variable that conveys tremor information back to the brain. Proprioception is compromised even in the early stages of Parkinson's Disease (PD), and may underlie several of the motor deficiencies in PD [5]. Using velocity-dependent force feedback to counter the tremor closes the loop on the brain's resting state oscillatory network controlling tremulous joints, and decreases the effect of this hyperkinetic state disturbance. Exploiting this channel to develop non-invasive therapies against tremor would avoid or delay the side effects of dopaminergic drugs prescribed to PD patients.

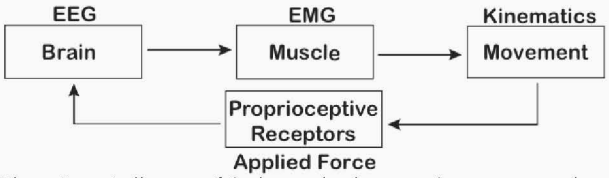

Figure 1. A diagram of the interaction between the motor control-observables in simplified form.

II. Methods

A. Subject

A 56 year-old female with idiopathic Parkinson's disease and mild, persistent resting tremor of the right hand was recruited for the study. The experiment was first conducted while the patient had been off of her dopaminergic therapy for 12 hours[6] The experiment resumed one hour after the patient took her anti-Parkinson's medications. The clinical severity of her right hand resting tremor on the United Parkinson's Disease Rating Scale[7] was 2.0 when she was off dopaminergic therapy, and 0.0 when she was on therapy (the scale ranges from 0.0 indicating an absence of tremor to 4.0 indicating marked, persistent tremor). The patient was seated comfortably in front of a table containing the haptic set-up with both arms parallel and resting upon a padded surface as shown in Fig. 2. The subject signed informed consent documents approved by the human subjects Institutional Review Board of the University of California, San Diego.

B. Proprioceptive Feedback

Force feedback was implemented using two Phantom Premium 1.0A haptic robots attached to the thumb and index fingers of the patient's right hand. The haptic robots allowed force to be applied with 3 degrees of freedom and also recorded position in Cartesian coordinates with sub-millimeter precision. The robots are designed for finger manipulation and contain safety mechanisms and force limits to prevent injury. Four different modalities were tested: a no-force control environment where the robots actively compensate for their own weight, a "low viscosity" environment where the patient experienced a counterforce to movement proportional to the velocity, a "high viscosity" environment where the scaling coefficient of the counterforce was greater, and a random noise environment where the fingers were subjected to a force with a constant magnitude

N. Govil is with the Institute for Neural Computation, University of California-San Diego, La Jolla, CA 92093 USA (nigovil@ucsd.edu).
A. Akinin is with the Department of Bioengineering at the University of California, San Diego, La Jolla, CA 92093 USA
S. Ward is with the Department of Radiology at the University of California-San Diego, La Jolla, CA 92093 USA (email: s1ward@ucsd.edu)
J. Snider is with the Institute for Neural Computation, University of California-San Diego, La Jolla, CA 92093 USA (email: j1snider@ucsd.edu)
M. Plank is with the Institute for Neural Computation, University of California-San Diego, La Jolla, CA 92093 USA (email: mplank@ucsd.edu)
G. Cauwenberghs is with the Institute for Neural Computation and the Department of Bioengineering at the University of California-San Diego, La Jolla, CA 92093 USA (e-mail: gert@ucsd.edu)
H. Poizner with the Institute for Neural Computation, University of California-San Diego, La Jolla, CA 92093 USA

but random direction. These modalities are compared in Table 1.

TABLE I. SENSORY FEEDBACK MODES

Conditions	*Magnitude (N)*	*Trials*[a]	*Duration (sec)*
No Force	0	2	120
Low Viscous	0.3*velocity[dm/s]	2	120
High Viscous	0.9*velocity[dm/s]	2	120
Random Noise	0.1	2	120

a. Trials were pseudorandomly ordered

C. *Electroencephalographic Recording.*

A 60 channel EEG signal from a flexible cap with active wet electrodes was recorded at a sampling frequency of 1,024 Hz using a Biosemi, Inc. ActiveTwo amplifier. Electrode locations and the shape of the patient's skull were digitized by electromagnetic localization (FASTRAK, Polhemus, Inc.). After the experiments, the EEG data was re-referenced to the average mastoid potential and band-pass filtered between 1Hz and 55Hz. Artifact rejection was performed using ICA-based analysis of the scalp potentials using EEGLAB [8] to remove the effect of eye blinks and local muscle activity.

D. *Electromyographic Recording.*

Seven channels of EMG were recorded at a sampling frequency of 1,024 Hz using an extension of the same amplifier mentioned in the previous section. Surface electrodes were placed in the following sites: Dorsal first digital webspace (first dorsal interosseous), the eminence (abductor pollicus brevis), wrist/finger flexors, wrist/finger extensors, elbow extensors (triceps), elbow flexors (biceps), all referenced to a ground electrode placed on the bare zone of the proximal ulna. Maximal voluntary force was measured for each muscle group. After experimentation the EMG data was bandpass filtered from 30Hz to 400Hz and then full wave rectified.

E. *Motion Capture Recording*

Positions of the chest, shoulder, and arm were recorded at 120 Hz using a 24 camera 3D tracking system (Phasespace, Inc.). Rigid body markers consisting of 4 LEDs on a planar surface were affixed to the dorsal surface of the hands, and to the chest to capture any rotations of these segments. LEDs were also taped to the wrists, elbows, and shoulders (Figure 2). Motion capture recording was performed to ensure that the patient did not make any significant body movements that would perturb the setup, and to monitor whether the tremor occurred at segments other than the fingers of the right hand (which it did not).

F. *Pre-processing*

The EEG data were first made reference-free using the Current Source Density Toolbox [9]. EEG and EMG data were collected and divided into epochs of 1s using EEGLAB. Epochs were discarded if the average rectified EMG value fell below a certain threshold. The threshold was determined from epochs with small kinematic activity to account for baseline noise and non-tremor EMG activity and was standardized for all trials. The results were confirmed by visual inspection.

Figure 2. Experimental setup

III. RESULTS

A. *Behavioral Analysis*

Analysis of the kinematics was performed by obtaining the absolute displacement of the thumb from the kinematic data recorded by the haptic robot. Kinematic data was filtered to remove drift of the patient over time. Fig. 3 shows the tremor activity on the patient's right thumb while the patient was off dopaminergic medication. Tremor presents itself sporadically with amplitudes exceeding 1cm peak-to-peak in the no-force condition. During force feedback, the tremor amplitude markedly decreased as expected. The high viscous condition had the lowest tremor amplitude. Kinematic data for the patient while on dopaminergic medication (see Fig. 4) showed no observable tremor activity in any of the trials.

The patient presented an altered awareness of the action of the robots within the different trials. When unmedicated, the subject was not able to recognize any random or viscous type force-feedback. After taking the medication, the patient

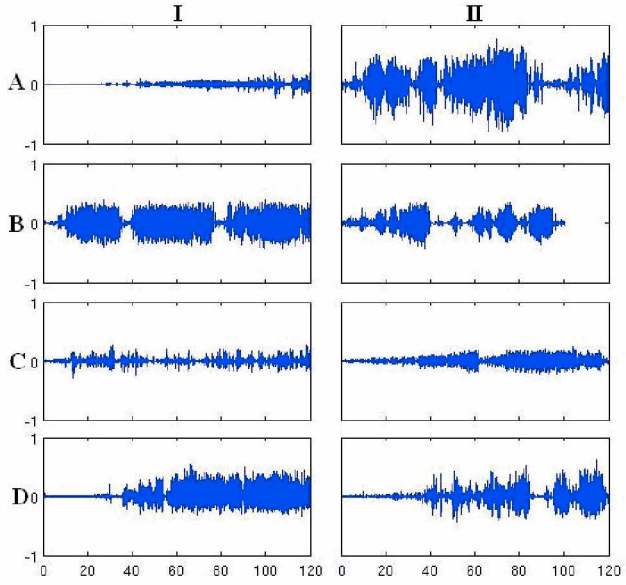

Figure 3. A depiction of typical tremor activity in the patient off medication in two trials (columns I-II) for the different force feedback conditions in the study: (A) No force applied, (B) Low-viscous force, (C) High-viscous force and (D) Random Noise force. The vertical axes show displacement (filtered to remove drift) from -1cm to 1cm, while the horizontal axes show the complete time of each trial, 120 sec.

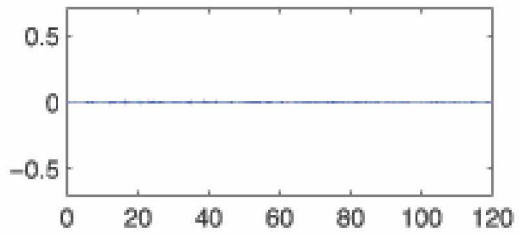

Figure 4. Displacement of the thumb for one trial while on medication in the no force condition. The vertical axis is in centimeters and the horizontal axis is the time of the trial, 120 sec. Subject had no noticeable tremor when on medication. Notice the different scale.

was able to perceive the force inputs from the random trial, but due to the lack of tremor was not able to experience a significant tremor modulation.

B. Coherence Analysis

The power spectral analysis of the EMG signal showed a dominant peak at the basic tremor frequency as well as at the first harmonic. As in [4], EEG-EMG coherence during tremor was significant at double the tremor frequency, more so over contralateral motor and somatosensory cortexes (Figure 3). In the force feedback conditions, the cortical area of coherence was larger and centered more posteriorly than during the no force and random conditions (Figure 7). The random noise condition had the lowest coherence among the four conditions, suggesting that uncorrelated proprioceptive input may reduce the strength of the EEG-EMG coherence.

IV. Conclusion

Although tremor genesis is a complex phenomenon, we have examined the behavior of Parkinsonian resting tremor under different force-feedback conditions. We were successfully

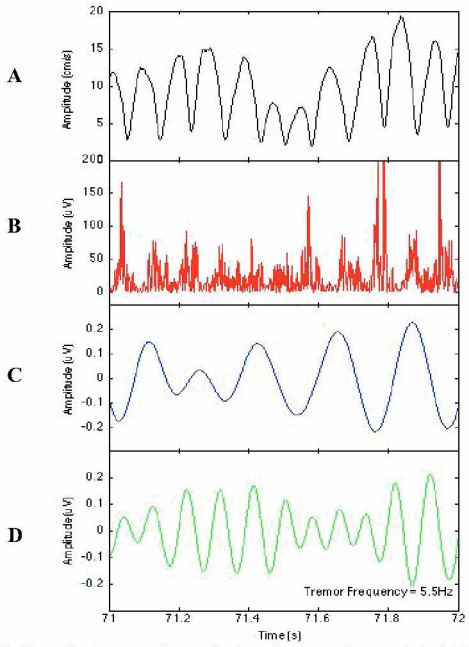

Figure 5. Sample 1-second epoch data from no force trial. (A)Thumb velocity (magnitude). (B) EMG of abductor pollicus brevis. (C) 5.5 Hz Wavelet of EEG Electrode C3. (D) 11 Hz Wavelet of EEG Electrode C3. EMG peaks occur at zeroes of thumb velocity as expected. The EEG Wavelets show phase synchrony with the EMG signal.

able to reduce the tremor amplitude using a viscous force feedback system. This, however, did not reduce the amplitude of the tremor EMG signal, nor did it modulate its frequency. Coherence between EEG and EMG channels during tremor was consistent with the literature [4] demonstrating maximal coherence at the first harmonic of the tremor frequency. However, we did not observe

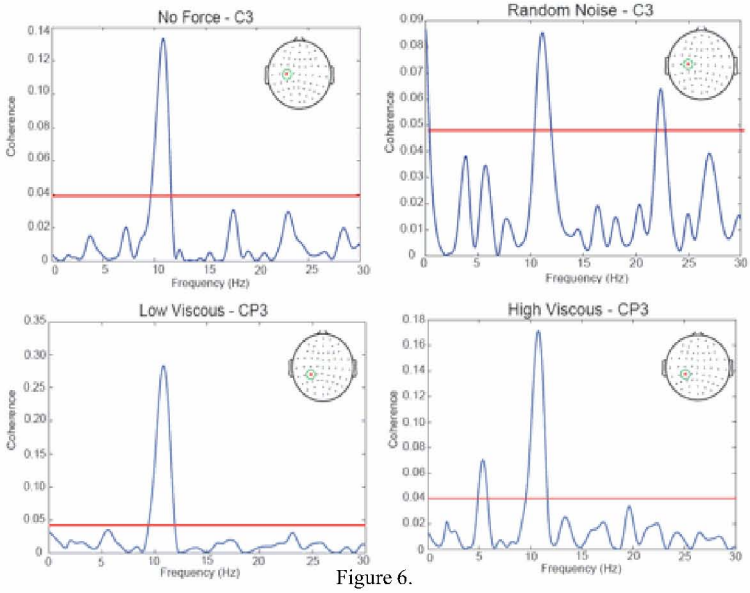

Figure 6.

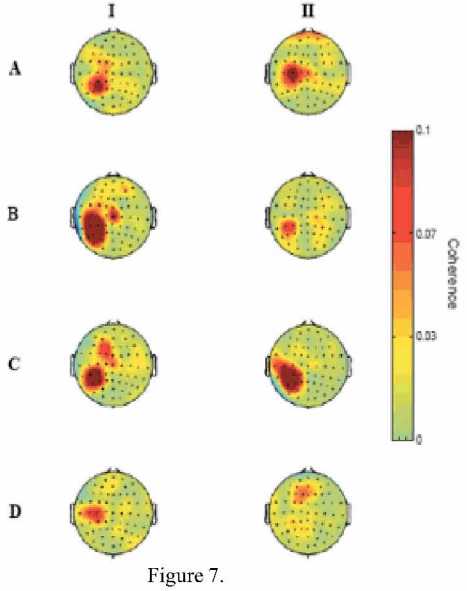

Figure 7.

Figure 6. (left): EEG-EMG coherence plots of the electrode with the highest coherence for each of the four conditions averaged across trials. The red line represents the 99% confidence level. Values above the line are significant at $p<0.01$. During the No Force and Random Noise conditions, the most coherent electrode was C3, which is located over the left (contralateral) motor cortex. During the viscous friction conditions, the most coherent electrode was CP3, located more posteriorly over the left somatosensory region. Note that the coherence plots have different scales. Figure 7. (right) Topographical scalp plots of coherence values at 11 Hz. Columns represent trials (I, II). Rows represent each condition: No Force (A), Low Viscous (B), High Viscous (C), Random Noise (D). Note the posterior shift to electrodes located over parietal cortex having the greatest EEG-EMG coherence in the viscous load conditions.

significant coherence at the basic tremor frequency in most trials. The posterior shift in the center of coherence during the viscous force feedback indicates greater activity over somatosensory and sensorimotor integration regions, in addition to the previously observed motor cortex activity.

Interestingly, the subject was not conscious of any force feedback from the robots while unmedicated, which may reflect impaired processing of proprioception information. Nonetheless, we measured changes in the EEG signal over somatosensory and sensorimotor integration cortices due to the force feedback we provided. Given the deep integration between sensory and motor cortices, there may be a training paradigm to reduce the severity of Parkinsonian tremor through a force feedback closed-loop system that over time would lead to plastic changes in tremor generating circuits. It would also be interesting to find the optimal-energy control strategy for reducing resting tremor with minimum loss of function.

V. Appendix

Coherence is the magnitude-squared of the cross-spectral densities normalized to the product of the auto-spectral densities. The coherence of two signals, x and y, (C_{xy}) was calculated using the following equation:

$$C_{xy} = \frac{|G_{xy}|^2}{G_{xx}G_{yy}} \quad (1)$$

where G_{xy} is the cross-spectral density and G_{xx} and G_{yy} are the auto-spectral densities of x and y, respectively. The confidence level (C.L.) of coherence was determined from:

$$C.L. = 1 - (1-\alpha)^{\frac{1}{L-1}} \quad (2)$$

where α is the confidence level and L is the number of samples [10].

Acknowledgment

Supported in part by NSF Grant EFRI-11372790, NIH Grant #2 R01 NS036449, NSF Grant #SBE-0542013 and ONR MURI Award No. N00014-10-1-0072. The authors thank Cheolsoo Park and Manuel Hernandez for their contributions to this project.

References

[1] L. Timmerman, J. Gross, M. Dirks et al, "The cerebral oscillatory network of parkinsonian resting tremor." *Brain*, vol. 126 iss. 1, pp. 199-212 July 2002

[2] E. M Jobges, J. Elek, J. D Rollnik et al. "Vibratory proprioceptive stimulation affects Parkinsonian tremor." *Parkinsonism & related disorders*, vol. 8 iss. 3, pp. 171-176, April 2001

[3] Spiegel, J, Fuss, G, Krick, C, et al. "Influence of proprioceptive input on Parkinsonian tremor." *Journal of clinical neurophysiology*, vol.19 iss.1, pp. 84-89, January 2002

[4] M. Muthuraman, U. Heute, K. Arning et al. "Oscillating central motor networks in pathological tremors and voluntary movements. What makes the difference?" *NeuroImage* vol. 60, iss. 2, pp. 1331-1339, January 2012

[5] J Konczak, DM Corcos, F Horak, H Poizner, M Shapiro, P Tuite, J Volkmann and M Maschke "Proprioception and Motor Control in Parkinson's Disease." Journal of Motor Behavior. Vol. 41, iss. 6, 2009.

[6] S. Fahn, R.L. Elton. UPDRS Program Members. Unified Parkinson's disease rating scale. In: Fahn S, Marsden CD, Goldstein M, Calne DB, editors. Recent developments in Parkinson's disease, Vol. 2. Florham Park, NJ: Macmillan Healthcare Information; p 153–163, 293–304. 1987

[7] G.L. Defer, H. Widner, R.M. Marie, P. Remy, M. Levivier. Core assessment program for surgical interventional therapies in Parkinson's disease (CAPSIT-PD). Mov Disord. 14(4): 572–84. 1999

[8] A Delorme & S Makeig. "EEGLAB: an open source toolbox for analysis of single-trial EEG dynamics," Journal of Neuroscience Methods. 134:9-21. 2004

[9] J. Kayser, C.E. Tenke. "Principal components analysis of Laplacian waveforms as a generic method for identifying ERP generator patterns: I. Evaluation with auditory oddball tasks." Clinical Neurophysiology, 117(2), 348-368, 2006

[10] D. R. Brillinger. *Time Series: Data Analysis and Theory*. Holt, Rinehart & Winston, New York. 1975